Biointerface Research in Applied Chemistry
Open-Access Journal (ISSN: 2069-5837)

Article
Volume 13, Issue 4, 2023, 363
https://doi.org/10.33263/BRIAC134.363

Nano-LC-FTMS Analysis of the Primary Structure and Post-translational Modifications of the α1 Subunit of the $GABA_A$ Receptor

Natalia Akentieva [1,*]

[1] Laboratory Biochemical and Cellular Studies, Department Kinetics of Chemical and Biological Processes, Institute of Problems of Chemical Physics Russian Academy of Sciences, Academician Semenov avenue 1, City Chernogolovka, Moscow Region142432, Russia; na_aken@icp.ac.ru (N.A.);
* Correspondence: na_aken@icp.ac.ru (N.A.);

Scopus Author ID 56370037400
Received: 20.05.2022; Accepted: 20.07.2022; Published: 24.09.2022

Abstract: $GABA_AR$ is one of the most significant drug targets in the treatment of neuropsychiatric disorders such as epilepsy, insomnia, anxiety, as well as anesthesia in surgical operations. However, complete information on the regulation of $GABA_A$ receptor activity is lacking. Therefore, studies are needed on post-translational modifications of receptor subunits that exhibit different pharmacological and physiological properties. $GABA_AR$ has been immunopurified from rat brain membranes on protein A agarose beads immobilized with complex anti-$GABA_AR$ antibody. Primary structure and post-translational modifications of the α_1 subunit of $GABA_AR$ have been characterized by nano-LC-FTMS peptide mapping by direct in situ–gel digestion on the one-dimensional gel. The primary structure of the α_1 subunit of $GABA_AR$ has been identified with high sequence coverage (81%, 371 from 455 amino acids). The extracellular domains, N-terminal and the C-terminus, have been identified with extensive sequence coverage, 85 and 100 % (214 from 249 amino acids), respectively. Other soluble domains, including the M1-M2 linker, and the M3-M4 linker, have also been determined with 100 and 85 % (75 from 88 amino acids), respectively. Transmembrane domains, including M1, M2, and M4, were identified almost completely. Post-translational modifications of the α1 subunit peptides have been found, such as phosphorylation, methionine oxidation, and carbamidomethylation.

Keywords: nano-LC-FTMS mass-spectrometry; sequence coverage; α1 subunit of $GABA_AR$; post-translational modifications.

1. Introduction

The $GABA_AR$, γ-aminobutyric acid receptor, is the major neurotransmitter inhibitor in the central nervous system (CNS) in the vertebrate brain. It belongs to a family of ligand-gated ion channels consisting of hetero oligomeric glycoprotein complexes in synaptic and extra-synaptic membranes [1-3].

Previously, $GABA_AR$ was isolated and purified by affinity chromatography from the brain of bovines, pigs, chickens, and rats [4-7]. The composition of the $GABA_AR$ subunits was examined by SDS-PAGE electrophoresis, and the results showed protein localization at 51-56 kDa. The identified 51 and 53 kDa proteins migrated together with the products of the α_1 and α_2 genes, shown using the Western blot method with subunit-specific antibodies [8,9]. Molecular biological studies have identified a large family of homologous GabR subunits

(named α, β, γ and δ) and subunit isoforms (α_1-α_6, β_1-β_4 and γ_1-γ_4), each of which is encoded by a separate *GabR* gene [10,11]. Using the partial purified $GABA_AR$, cDNA encoding the bovine α_1, α_2, α_3, α_4, α_5 and α_6 subunits of the $GABA_AR$ has been isolated [12-14]. It has been shown that long mature protein contains an exceptionally long intracellular domain [14]. Later, human $GABA_AR$ α_2 and α_3 cDNAs were cloned and sequenced [14,15]. Their deduced amino acid sequences showed much sequence identity with the published bovine sequences (98.2 % and 97.0 % for α_2 and α_3, respectively). It was shown that there is a significant similarity between the deduced amino acid sequences of all α subunits, especially in the predicted four transmembrane regions of the molecules [16,17]. Thus, $GABA_AR$ has been shown to contain many different isoforms of the α-subunits; they have a similar amino acid sequence but are likely to have a number of post-translational modifications that are important in regulating their activity. Such a huge variety of $GABA_AR$ subunit isoforms can be explained by different molecular mechanisms of regulation. It should be noted that the cloned sequence of the $GABA_AR$ gives the complete amino acid sequence but does not allow the identification of post-translational modifications of subunit isoforms. At the same time, characterization of post-translational modifications is important and necessary for understanding cell signal transduction in the CNS and the molecular mechanism of regulating $GABA_AR$ activity. It is now known that mass spectrometric mapping of peptides is a very sensitive and accurate method for characterizing the primary structure of proteins. In addition, mass spectrometry has been recognized for decades as an important technology for analyzing different post-translational modifications, such as protein phosphorylation, glycosylation, sulfonation, acetylation, and methylation of modified peptides. Among many mass spectrometric methods, the nano-LC-FTMS is the most rapid, accurate, and efficient tool to sequence proteins and identify post-translational modifications from small amounts of tissues with high sensitivity and speed [18,19].

Previously, the expression of a combination of subunits in *Xenopus oocytes* of transfected mammalian cells showed that α, β, and γ subunits are required for the formation of $GABA_AR$ with the expected properties [20,21]. In addition, the functional heterogeneity of the $GABA_AR$ complex has been suggested based on the pharmacological characterization of the receptor using electrophysiological and radio-ligand binding assays [22,23].

The predominant $GABA_AR$ in the cerebral cortex consists of α- and β-subunit polypeptides that bind GABA (or $GABA_A$ agonists, muscimol, and isoguvacine) and benzodiazepines (flunitrazepam and diazepam, respectively) [24-28]. Two discrete binding sites in the M1 and M4 transmembrane domains of $GABA_AR$ (chimera mouse and *Drosophila*) have also been identified that mediate neurosteroids' potential and direct activating effects [29]. Using the method of site-directed mutagenesis, it was shown that the amino acids αThr 236 (M1) and βTyr 284 (M4) initiate activation, while the amino acids αGln 241 (M1) and αAsn 407 (M4) mediate an increase in responses to GABA or neurosteroids [29]. These data indicate that the neurosteroid binding site may be located on the α_1 subunit of $GABA_AR$. However, the problem is that site-directed analysis provides ambiguous explanations for interpreting the results. Therefore, it would be important to have a fast, convenient and accurate mass spectrometry approach for peptide mapping of proteins and receptors. Sequence comparison of labeled and unlabeled peptides will allow identification of amino acid residues and study of the structure of the ligand binding site. In this case, using nano-LC-FTMS in combination with the

photolabeling approach can become a promising and direct tool for studying the structure of ligand-binding regions of receptors and proteins.

This study aimed to isolate and purify $GABA_AR$ from a small amount of rat brain tissue and to identify the amino acid sequence and post-translational modifications of the $GABA_AR$ α_1 subunit using nano-LC-FTMS analysis.

2. Materials and Methods

2.1. Materials.

In the work we used reagents for the qualification of analytical grade. Rat brains containing the $GABA_AR$ (*Rattus norvegicus*) were purchased from Pel-freez (USA) and used to prepare membranes. SDS-PAGE reagents, SDS-PAGE purification kit, and Western blotting reagents were from Amersham Biosciences (USA) and Calbiochem (USA). The Sypro Ruby protein staining kit was purchased from Invitrogen (USA). A complex of anti-$GABA_AR$ antibodies (directed against α_1, β_1, β_2, β_3 and γ_2 subunits) were purchased from Antibodies Inc., Davis (USA). Goat anti-rabbit IgG-HRP antibodies for Western blotting were purchased from Santa Cruz Biotechnology (USA). Centricon Plus-20 membrane was from Millipore (USA), and protein A agarose was purchased from Sigma (USA). Immuno-blot ^{TM}PVDF membrane was purchased from Bio-Rad (USA).

2.2. Membrane preparation.

The membranes from rat brain regions were isolated, as described in the article [30]. Frozen areas of the brain of rats were homogenized in a solution of sucrose (0.32 M) and then centrifuged for 10 min at 1000 g at a temperature of 0-4°C. After that, the resulting supernatant was centrifuged at 100,000 g for 45 min. The resulting precipitate was then osmotically destroyed in distilled water, and then washed twice with membrane washing buffer and stored frozen.To prepare the lysate, the membranes were thawed, precipitated, and washed twice with buffer (20 mM K_2HPO_4/KH_2PO_4 buffer with 50 mM KC1, pH 7.5). Membranes were prepared by centrifugation at 100,000 g for 20 min, then the membranes were washed once with membrane wash buffer and resuspended in lysis buffer (10 mM Tris-HCl buffer with 150 mM NaC1, pH 8.5, 0.05% phosphatidylcholine, 0.5 % Na-Deoxycholate, 1 complete protease inhibitor cocktail tablet), to obtain the final protein concentration (1 mg/ml), and then incubated for 60 min at 40°C. The resulting suspension was then centrifuged at 16,000 x g, and the supernatant (lysate) was loaded on the protein A gel column for immunopurification.

2.3. Immunopurification of $GABA_AR$.

α_1 subunit of $GABA_AR$ was isolated from rat brain membranes (RBM) and purified by the method of immunoaffinity chromatography with some modifications [31]. The lysate from RBM was applied to a column consisting of a complex of anti-$GABA_AR$ antibodies (directed against α_1, β_1, β_2, β_3 and γ_2 subunits), coupled to Protein A agarose beads. The column was washed with three volumes of triton buffer (50 mM Tris-HCl, 1 mM EDTA, 0.1 % Triton X-100, pH=8.3), six volumes of immunoprecipitation (IP) high buffer (50 mM Tris-HCl, 0.6 M NaCl, 1 mM EDTA, 0.5 % Triton X-100, pH=8.3) and six volumes of IP low buffer (50 mM Tris-HCl, 150 mM NaCl, 1 mM EDTA, 0.2 % Triton X-100, pH=8.3) and was eluted with glycine buffer (0.1 m Glycine-HCl, 150 mM NaCl, 0.1 % Triton X-100, pH=2.45). Eluate has

been neutralized with 1 M Tris, pH-9.0. The $GABA_AR$ solution concentrated on Centricon Plus 20 membrane. Before electrophoresis, the $GABA_AR$ was precipitated with an SDS-PAGE clean-up kit, and the pellet was dissolved in sample buffer (62.5 mM Tris-HCl, pH=6.8, 10 mM EDTA, 10 % (v/v) glycerol, 2 % SDS, 0.002 % bromphenol blue and 5 % dithiothreitol, pH=6.8) for SDS-PAGE.

2.4. Measurement of the amount of $GABA_AR$.

The presence of $GABA_AR$ was measured by RO15 assay, which shows the benzodiazepine binding site on the surface between α_1 and γ_2 subunits [32].

2.5. Electrophoresis.

Polyacrylamide gel electrophoresis (10% polyacrylamide gel under reducing conditions) was used for protein analysis [33]. After electrophoresis, the gels were stained or used for Western blot analysis. Gels were Sypro Ruby stained with the kit.

2.6. Western blot analysis.

For Western blotting, proteins from SDS-PAGE gels were transferred to a Tropifluor™ polyvinylidene difluoride membrane. The membrane was then treated with 5% milk powder for 1 hour to block non-specific binding, after which the membrane was washed three times with Tris-buffered saline containing Tween 20 (0.05%) and incubated overnight with primary the anti-γ_2 subunit $GABA_AR$ mAb (rabbit) (1:2000). Then the membranes were washed three times again with Tris-buffered saline containing Tween 20 (0.05%) and incubated with goat anti-rabbit IgG –HRP (1:20 000) for 1 h. An ECL-plus Western blotting system was used to detect immunoreactive bands.

2.7. Digestion in the SDS-PAGE matrix (in situ gel digestion).

For proteolytic cleavage of proteins in SDS gel matrix, the following method was used [34,35]. Staining and decolorizing the gel were carried out quickly since both steps lead to partial fixation of the proteins in the gel. Protein bands were then excised from the gel using robotic instruments, and the gels were washed for 1 hour in 40% (v/v) aqueous acetonitrile to remove the residual dye, buffer, and SDS. The cleaned gel pieces were dried at room temperature in a vacuum, in a centrifuge, and soaked until swollen in a solution (100 µl of 50 mM NH_4HCO_3 containing 12.5 ng/µl of modified trypsin) in an ice bath. After the gel pieces had reached their original size, the supernatant was removed, and a solution (100 µl of 50 mM NH_4HCO_3) was added. Proteolytic cleavage of proteins in the gel was carried out with trypsin for 24 h at 37°C with gentle shaking. Then the resulting peptides were extracted with a mixture of acetonitrile and 50 mM NH_4HCO_3 (1:1) for 24 h and lyophilized. The lyophilized powders were dissolved in UHQ water, and the peptides were precipitated by adding 10% TCA. After that, the samples were centrifuged for 10 min at 15,000 g at 0°C. Then, after precipitation, it was washed with cold acetone, dried, and stored at –20°C.

2.8. Nano-LC-FTMS analysis.

Mass spectrometry was performed using a mass spectrometer with a quadrupole ion trap and Fourier transform ion cyclotron resonance (LTQ-FTMS, Thermoelectron, USA). The nano-liquid chromatograph (Eksigent nano-LC, USA) was interfaced to the LTQ-FTMS with

a Pico-View nano-capillary source from New Objective (USA). Samples were injected using an autosampler (Endurance, USA) into a column, which was a PicoFrit C-18 (75 μm × 10 cm) (New Objective, USA). Water for HPLC (Fisher Scientific, USA) containing 1% formic acid (Sigma-Aldrich, USA) (Solvent A) and acetonitrile (Burdick & Jackson, USA) containing 1% formic acid (Solvent B) were used as mobile phases. The sample (5 μl) was applied at a rate of 600 nl/min at 1% B for 10 min.

Then the flow rate was reduced to 200 nl/min with isocratic elution for 20 minutes, followed by a linear increase in solvent B (2%/min) over 40 minutes.
The LTQ-FTICR (7 T) mass spectrometer was configured to operate in a data-dependent mode. Overview scans (m/z = 450-1500) were obtained using FTICR-MS with a resolution of ~100,000 at m/z = 421.75 after the accumulation of ions in the trap to a value of ~1,000,000. The 10 most abundant ions were isolated and analyzed after reaching a target value of ~40,000. An insulation width MS/MS of 2.5 Da was used, and the normalized collision energy was 35%. Electrospray ionization was carried out at a sputtering voltage of 2.8-3.1 kV without a gas envelope. The temperature of the ion exchange tube was 200°C.

2.9. MS data analysis.

Theoretical unmodified peptide mass lists for α_1 $GABA_AR$ (NP_899151) were obtained by *in silico* theoretical trypsin digestion using Protein Prospector (http://prospector.ucsf.edu)[29,36]. The missing trypsin cleavages (0-8) and the following variable modifications were taken into account: acetylation (N-terminus), cysteine carbamidomethylation (C), methionine oxidation (M), pyro-glu (N-terminus Q), and serine phosphorylation. as well as threonine and tyrosine residues. The acquired MS data were collected in profile mode, as were the MS/MS spectra [37,38]. “Raw” files were analyzed using LCQ-DTA software (Thermoelectron) and then the resulting files were exported to MASCOT 1.9.05 software (Matrix Science, UK). The following LCQ-DTA settings were applied: grouping tolerance 0.0001 Da; "intermediate scans" (1); and "minimum number of scans per group" (1). The following settings and databases were used to search for tandem MS data (taking into account 0, 1, 2, 3, or 5 missed trypsin digestions): (1) enzyme, trypsin, MS tolerance 3 ppm, MS/MS tolerance 0.8 Da, and carbamidomethylation of cysteines and methionine oxidation as "variable modifications"; (2) lack of enzyme, MS tolerance 3 ppm, MS/MS tolerance 0.8 Da, α_1 subunit of $GABA_AR$ (NP_899151) and carbamidomethylation of cysteines, oxidation of methionines and phosphorylation of all serine, threonine and tyrosine residues in the form of variable modifications [39]. MS/MS spectra were searched against the rat database (*Rattus norvegicus*).

3. Results and Discussion

3.1. Immunopurification of $GABA_AR$.

$GABA_AR$ has been immunopurified on protein A agarose column, containing the complex anti-$GABA_AR$ antibody, directed against α_1, β_1, β_2, β_3 and γ_2 subunits, $GABA_AR$ has been eluted by glycine and amount of receptor has been measured by Ro15 assay. The Ro15 assay shows the benzodiazepine binding site on the surface between α_1 and γ_2 subunits. The lysate (unpurified sample) showed 19.5 pmol binding by Ro15 assay, and the IP (immunopurified) eluant contained 5.8 pmol bindings. The purification procedure, including

one step on protein A agarose column, did differ significantly from the protocols described in the literature. After immunopurification, the lysate and IP eluent samples were loaded on an SDS-PAGE gel. Protein profiles from rat brain membranes are shown in Figure 1 (a).

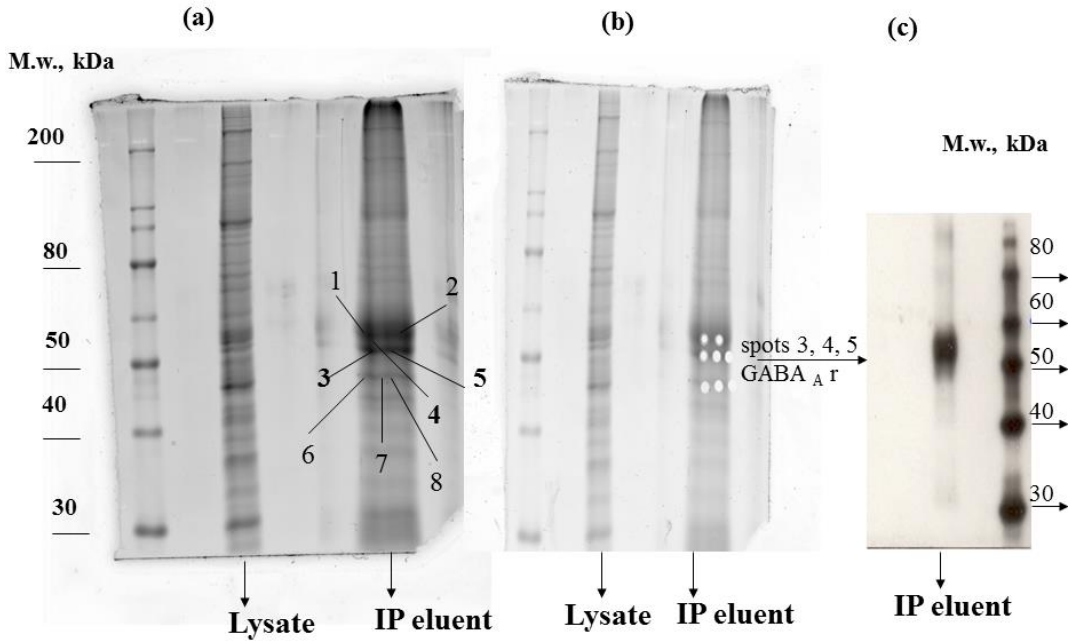

Figure 1. Gel profiles of $GABA_AR$ obtained from RBM and presented for mass spectral analysis. (**a**) proteins stained with Sypro Ruby; (**b**) protein samples cut with robotic instruments, the cuts shown 1-8 (**c**) cross-reactivity of bands of proteins interacting with the anti-γ_2 antibodies. Marker proteins (with their molecular weight in kDa) are listed on the left. Numbers (3, 4, 5) show the localization of the $GABA_AR$ subunits.

A comparison of lysate and IP eluent samples showed that $GABA_AR$ has been purified completely and produced one major band around 52 kDa. This major protein band at 52 kDa was found to cross-react with antibodies directed against γ_2 subunits of $GABA_AR$ in these membranes, as detected by Western blot analysis (Figure 1, c). Other subunits of $GABA_AR$ are also co-immunoprecipitated during immunopurification. Localization of α and β subunits in this protein band has also been detected by Western blot analysis (data not shown). The main protein band of 52 kDa was selected, and the spots were cut out with a robotic tool (Fig. 1b). Then, gel bands were subjected to *in-gel* tryptic digestion. Peptides from gel bands were extracted by acetonitrile. Then peptides were analyzed by nano-LC-FTMS analysis.

3.2. Nano-LC-FTMS Analysis of subunits of the $GABA_AR$.

Analysis of the digests of spots 3, 4, and 5 using nano-LC-FTMS definitively identified the presence of the α_1, α_2, α_5, β_2, β_3, and γ_2 subunits of $GABA_AR$. Our initial work has focused on obtaining the sequence of α_1 subunit and determination of post-translational modifications. In this study, each nano-LC-FTMS analysis produced –6000-12 000 MS/MS spectra in the data-dependent mode. We explored the usefulness of searching for MS/MS spectra of $GABA_AR$ peptides in this large dataset using accurate mass measurements from the FTICR spectra. We determined an overlap (within 5 ppm) of m/z values (+1, +2, +3, +4, and +5 charge states) for tryptic peptides (0.1-8 missing cleavages) and variable modifications for cysteine urea methylation, oxidation of methionines and phosphorylation of all serine, threonine and tyrosine residues for α_1 subunit of $GABA_AR$ from rat brain. In addition, we then performed selected ion extraction analysis and analyzed spectra that contained signals corresponding to

the overlapping values. The MS/MS spectra were searched against the rat database. It was shown that the MS/MS signal spectrum of high quality (m/z value) refers to peptides of α_1 subunit. Then using selective ion chromatograms, we then analyzed all possible theoretical m/z values for 1-, 2-, 3-, 4-, and 5-charged peptides. Hence, using selected ion extraction, we analyzed the FTMS spectra according to the exact masses of α_1 subunit peptides in +1, +2, +3, +4, or +5 charge states. In addition, all FTMS spectra containing signals corresponding to these exact m/z values were then checked manually to confirm the theoretical charge value and isotope distribution.

3.3. MS data analysis.

Mass spec analysis data of the α_1 subunit peptides are presented in Table 1.

Table 1. Identification of peptides of the α_1 subunit of the $GABA_AR$ by nano-LC-FTMS.

SEQUENCE DOMAIN	START-END	SEQUENCE	THEORETICAL MASS	OBSERVED MASS	TANDEM	MODIFICATION
N-terminus	0-2	no covered peptides				
	3–24	KSRGLSDYLWAWTLILSTLSGR	731.5638	731.5762	no	5PO4
	15-36	TLILSTLSGRSYGQDELKD	2407.2082	2407.223	yes	
	25-43	SYGQPSQDELKDNTTVFTR	1093.522	1093.5225	yes	
	25-47	SYGQPSDELKDNTTVFTRILDR	539.0699	539.0632	yes	
	44-55	ILDRLLDGYDNR	731.8866	731.8876	yes	
	48-55	LLDGYDNR	964.4654	964.4614	yes	
	55-62	RLRPGLGE	896.5254	896.5191	yes	
	56-63	LRPGLGER	897.527	897.5191	yes	
	64-93	VTEVKTDIFVTSFGPVSDHDMEYTIDVFFR	749.7456	749.7417	yes	3PO4
	69-97	TDIFVTSFGPVSDHDMEYTIDVFFRQSWK	735.3461	735.3457	yes	
	93-118	RQSWKDERLKFKGPMTVLRLNNLMAS	3175.7182	3175.6746	yes	
	103-111	FKGPMTVLR	1063.5854	1063.5848	yes	1 met-ox
	105-111	GPMTVLR	894.4054	894.4034	yes	
	109-114	VLRLNNL	882.5254	882.5287	yes	
	112-119	LNNLMASK	905.4719	905.464	yes	1 met-ox
	120-132	IWTPDTFFHNGKK	530.9409	530.9404	yes	
	120-143	IWTPDTFFHNGKKSVAHNMTMPNK	563.4775	563.4685	no	
	133-143	SVAHNMTMPNK	957.932	957.9296	yes	
	135-151	AHNMTMPNKLLRITEDG	1981.9854	1981.9713	yes	
	147-158	ITEDGTLLYTMR	1427.7054	1427.6966	yes	1 met-ox
	159-160	no covered peptides				
	161-179	VRAECPMHLEDFPMDAHAC	2285.9482	2285.9326	yes	
	163-182	AECPMHLEDFPMDAHACPLK	1127.992	1127.99	yes	
	163-182	AECPMHLEDFPMDAHACPLK	762.9939	762.9982	yes	2 met-ox
	163-182	AECPMHLEDFPMDAHACPLK	572.4974	572.4948	yes	2 met-ox
	183-190	FGSYAYTR	963.4554	963.445	yes	
	191-199	AEVVYEWTR	1151.5654	1151.5611	yes	
	191-203	AEVVYEWTREPAR	1604.7982	1604.7946	yes	
	204-213	SVVVAEDGSR	1017.5054	1017.509	yes	
	214-247	no covered peptides				
M1,M1-M2 Linker	248-275	KIGYFVIQTYLPCIMTVILSQVSFWLNR	671.3389	671.3293	no	
M1,M1-M2 Linker	249-275	IGYFVIQTYLPCIMTVILSQVSFWLNR	1301.024	1301.014	yes	1 CAM-c 1 met-ox
M1,M1-M2 Linker	248-275	IGYFVIQTYLPCIMTVILSQVSFWLNR	802.4271	802.4308	yes	6PO4
M2	276-300	ESVPARTVFGVTTVLTMTTLSISAR	685.8239	685.825	yes	
M2	284-296	FGVTTVLTMTTLS	1427.7082	1427.7218	yes	
	300-338	no covered peptides				
M3-M4 Linker	339-346	RGYAWDGK	951.4654	951.4562	yes	
	347-354	SVVPEKPK	442.2666	442.2657	yes	
	356-362	VKDPLIK	406.7663	406.7663	yes	
	363-380	KNNTYAPTATSYTPNLAR	1981.9882	1981.9857	yes	
	364-380	NNTYAPTATSYTPNLAR	1853.8854	1853.8908	yes	
	381-390	GDPGLATIAK	941.5254	941.5182	yes	
	391-397	no covered peptides				
	398-409	EVKPETKPPEPK	1377.7582	1377.7503	yes	
	409-420	KTFNSVSKIDR	1293.6982	1293.7041	yes	1met-ox
M4	421-444	LSRIAFPLLFGIFNLVYWATYLNR	744.0781	744.0934	no	
C-terminus	424-455	IAFPLLFGIFNLVYWATYLNREPQLKAPTPHQ(-)	960.9458	960.9451	no	

Table 1 shows peptides that were observed using both precise mass determination and MS/MS spectra to determine the peptide sequence of the $GABA_AR$ of the α_1 subunit from RBM. Moreover, Table 1 compares the theoretical and calculated masses of the α_1 subunit peptides produced after digestion with trypsin and analysis using nano-LC-FTMS. Using the Protein Prospector program (http://prospector.ucsf.edu), the theoretical masses of peptides of the α_1 subunit were determined. Using the MASCOT search program, we determined the calculated masses of peptides of the (1 subunit as one-, two-, three-, four-, and five-charged ions.

Thus, the amino acid residues of the α_1 subunit were found by mass spectrometric analysis, based on the accurate mass determination, isotopic distribution, and tandem analysis.

Analysis of accurate masses from nano-LC-FTMS yielded 81 % (371 from 455 amino acids) total sequence coverage of the α_1 subunit. Some peptides (47 % of sequence, 214 from 455 amino acids) were abundant and definitively identified from tandem fragmentation spectra. Some peptides were not selected for tandem analysis because of low abundance. Post-translational modifications of the α_1 subunit peptides have been found, such as phosphorylation, methionine oxidation, carbamidomethylation (Table 1, Table 2).

Table 2. Identification of the post-translational modifications peptides of the α_1 subunit of the $GABA_AR$. (●) shows post-translational modifications of peptides: phosphorylation, methionine oxidation, and carbamidomethylation.

Start-end	Sequence	Start-end	Sequence	Start-end	Sequence
1-10	MKKSRGLSDY	181-190	LKFGSYAYTR	361-370	IKKNNTYAPT
11-20	LWAWTLILST	191-200	AEVVYEWTRE	371-380	ATSYTPNLAR
21-30	LSGRSYGQPS	201-210	PARSVVVAED	381-390	GDPGLATIAK
31-40	QDELKDNTTV	211-220	GSRLNQYDLL	391-400	SATIEPKEVK
41-50	FTRILDRLLD	221-230	GQTVDSGIVQ	401-410	PETKPPEPKK
51-60	GYDNRLRPGL	231-240	SSTGEYVVMT	411-420	TFNSVSKIDR
61-70	GERVTEVKTD	241-250	THFHLKRKIG	421-430	LSRIAFPLLF
71-80	IFVTSFGPVS	251-260	YFVIQTYLPC	431-440	GIFNLVYWAT
81-90	DHDMEYTIDV	261-270	IMTVILSQVS	441-450	YLNREPQLKA
91-100	FFRQSWKDER	271-280	FWLNRESVPA	451-455	PTPHQ
101-110	LKFKGPMTVL	281-290	RTVFGVTTVL		
111-120	RLNNLMASKI	291-300	TMTTLSISAR		
121-130	WTPDTFFHNG	301-310	NSLPKVAYAT		
131-140	KKSVAHNMTM	311-320	AMDWFIAVCY		
141-150	PNKLLRITED	321-330	AFVFSALIEF		
151-160	GILLYTMRLT	331-340	ATVNYFTKRG		
161-170	VRAECPMHLE	341-350	YAWDGKSVVP		
171-180	DFPMDAHACP	351-360	EKPKKVKDPL		

Most of them have been identified in extracellular soluble parts of the $GABA_AR$, especially in N-terminus, M1-M2-linker, and M3-M4 linker (Table 1). Three peptides were identified with the phosphorylated residues. We detected the two phosphopeptides in N-terminus, one $_3$KSRGLSDYLWAWTLILSTLSGR$_{24}$ with five phosphorylated residues, the second $_{64}$VTEVKTDIFVTSFGPVSDHDMEYTIDVFFR$_{93}$ with three PO_4 residues. In addition, we also identified the phosphopeptide in the M1 transmembrane domain, $_{248}$KIGYFVQTYLPCIMTVILSQVSFWLNR$_{275,}$ with six phosphorylated residues. Identifying phosphorylation sites on the (1 subunit is thought to confer the role of protein kinase in regulating the $GABA_AR$ activity.

Transmembrane domains M1, M2, and M4 peptides were found as 3+, 4+, and 5+ charged species. Some have been identified by the tandem analysis, some not, because of low abundance and high molecular masses. The high molecular masses of transmembrane domains demand to use of more energy for fragmentation collision reaction to cleavage peptides on amino acid residues. MS/MS spectra have been analyzed for each peptide. Eluted peptides were analyzed by the MASCOT search program. The total liquid chromatography spectrum of the

α_1 subunit of the $GABA_AR$ is shown in Figure 2 (a).

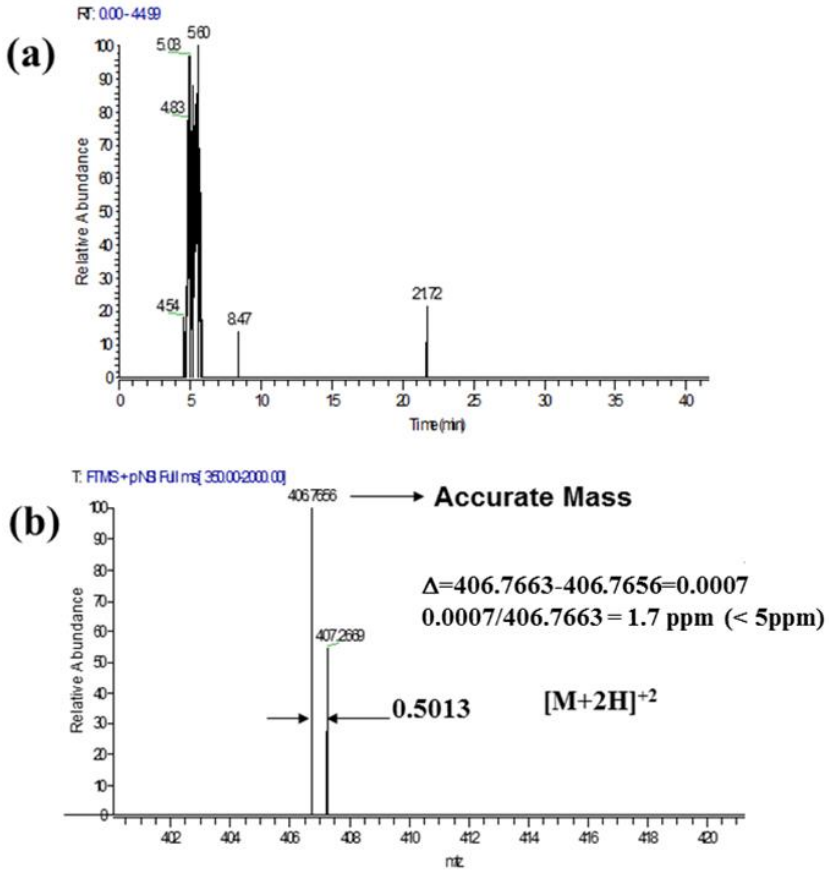

Figure 2. Nano-LC-FTMS analysis of tryptic digestions of the α_1 subunit of the $GABA_AR$ from RBM: (**a**), selected ion chromatogram of $_{356}$VKDPLIK$_{362}$ peptide from nano-LC-FTMS analysis of a tryptic digest of the α_1 subunit of the $GABA_AR$. The predicted theoretical mass of peptide (*m/z*) is 406.7663. (**b**), FTICR partial spectrum of $_{356}$VKDPLIK$_{362}$ peptide. Observed accurate mass=406.7656, the isotopic distribution is 0.5013. This peptide is a doubly charged ion, resolved ions in the isotope cluster are seen at *m/z* intervals of 0.5 Th, which is 1.0 Da divided by the charge of two Delta=406.7663-406.7656=0.0007, tolerance=0.0007/406.7663 = 1.7 ppm (< 5ppm).

As an example, in Figure 2(b) shows the MS/MS spectrum of the peptide which eluted after 4.88 minutes. The predicted theoretical mass of this peptide (406.7663) corresponds to a doubly charged state with the amino acid sequence $_{356}$VKDPLIK$_{362}$. The isotopic distribution (407.2669-406.7656) is 0.5013, which correlates with the double charge state of the peptide. Then we calculated the delta value (the difference between the theoretical and experimental mass (406.7663-406.7656=0.0007). The resulting delta value (0.0007/406.7663) divided by the theoretical mass indicates a tolerance of 1, 7 ppm, which is less than 5 ppm for this particular peptide.All peptides with a tolerance of less than 5 ppm were chosen by us as peptides corresponding to the predicted sequences. We compared the experimental MS/MS spectra with the fragmentation of the theoretical pattern found in Prospector. As can be seen from Figure 3, the MS/MS spectrum of this peptide showed an almost complete set of y- and b-ions, which corresponds to the theoretical amino acid sequence of the peptide. In addition, the complete set of b-(b_2-b_6) and y-ions (y_1-y_6) for interpreting of the sequence $_{356}$VKDPLIK$_{362}$ sequence is shown in Figure 3.

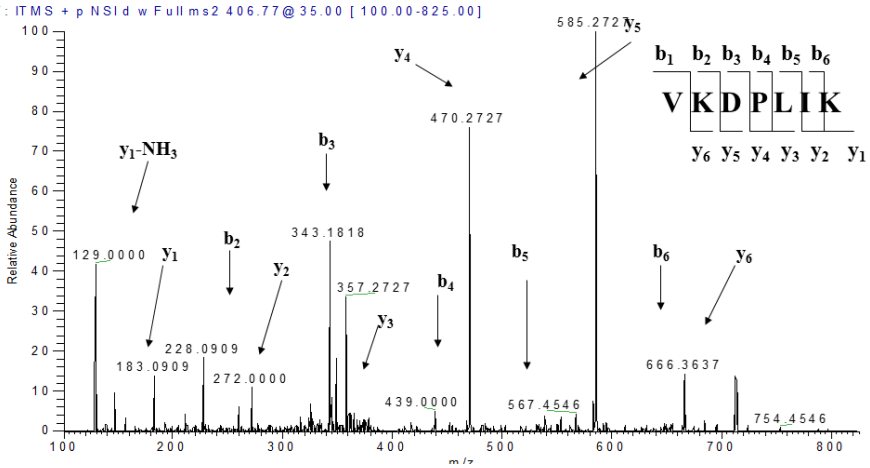

Figure 3. MS/MS fragmentation spectrum of the $[M+2H]^{2+}$ ion=406.7656 with t_r=4.88 min from $_{356}$VKDPLIK$_{362}$ acquired by nano-LS-FTMS. The complete list of theoretically assigned ions is given in Table 3.

It should be noted that we were not detected b_1-ion because of its low molecular mass. But the a-, b-NH_3, and y-NH_3 ions were determined. The list of theoretical patterns of fragmentation ions has given in Table 3.

Table 3. The theoretical pattern of fragmentation ions of the peptide $_{356}$VKDPLIK$_{362}$. Bold shows ions observed in MS/MS spectrum.

Sequence: **VKDPLIK** PARAMETERS
Amino Acid Composition: **D1 I1 K2 L1 P1 V1**
Peptide N terminus: **Hydrogen**
Peptide C terminus: **Free Acid**
User AA Formula 1: **C2 H3 N1 O1**
Cysteine Modification: **unmodified**
Instrument Name: **MALDI-TOF**
Ion Types Considered: **a, b, y, l, h, n, B**
Elemental Compositon: C38 H70 N9 O10
All fragment ion masses below are calculated as: **monoisotopic**masses
Peptide Mass MH+(monoisotopic): **812.5246**
Peptide Mass MH+(average): **813.0346**

MS-Product in ProteinProspector 4.0.6
© Copyright (1995-2005) The Regents of the University of California.

(MH)+2(average): 407.02
(MH)+2(monoisotopic): 406.77

65.55+2	y_1-NH_3+2	198.12+2	a_4-NH_3+2	263.17+2	a_5+2	341.18	KDP	525.34	a_5
74.06+2	y_1+2	199.18	LI-28	268.66+2	b_5-NH_3+2	342.72+2	b_5+H_2O+2	536.31	b_5-NH_3
92.08+2	a_2-NH_3+2	200.18	a_2	277.17+2	b_5+2	**343.20**	**b_3**	539.36	KDPLI-28
100.59+2	a_2+2	206.63+2	a_4+2	284.67+2	y_5-NH_3+2	348.72+2	y_5-NH_3+2	550.32	KDPLI-NH_3
106.08+2	b_2-NH_3+2	211.14	b_2-NH_3	286.18+2	b_5+H_2O+2	356.25	y_3-NH_3	**553.33**	**b_5**
114.59+2	b_2+2	211.14	PL	293.18+2	y_5+2	357.23+2	y_6+2	567.35	KDPLI
122.09+2	y_2-NH_3+2	212.12+2	b_4-NH_3+2	296.23	PLI-28	**373.28**	**y_3**	568.33	y_5-NH_3
130.09	y_1-NH_3	213.09	DP	298.18	DPL-28	395.23	a_4-NH_3	571.35	b_5+H_2O
130.60+2	y_2+2	216.13	KD-28	298.18	a_3-NH_3	411.26	DPLI-28	**585.36**	**y_5**
147.11	**y_1**	220.63+2	b_4+2	311.20+2	a_5-NH_3+2	412.26	a_4	621.40	a_6-NH_3
149.59+2	a_3-NH_3+2	227.10	KD-NH_3	313.19	KDP-28	423.22	b_4-NH_3	638.42	a_6
158.11+2	a_3+2	227.16+2	y_4-NH_3+2	315.20	a_3	426.27	KDPL-28	649.39	b_5-NH_3
163.59+2	b_3-NH_3+2	227.18	LI	319.72+2	a_5+2	437.24	KDPL-NH_3	**666.42**	**b_6**
172.10+2	b_3+2	**228.17**	**b_2**	324.16	KDP-NH_3	439.26	DPLI	684.43	b_5+H_2O
178.63+2	y_3-NH_3+2	235.67+2	y_4+2	324.23	PLI	**440.25**	**b_4**	696.43	y_6-NH_3
183.15	a_2-NH_3	243.17	y_2-NH_3	325.20+2	b_5-NH_3+2	453.31	y_4-NH_3	**713.46**	**y_6**
183.15	PL-28	244.13	KD	326.17	b_3-NH_3	454.27	KDPL		
185.09	DP-28	254.66+2	a_5-NH_3+2	326.17	DPL	**470.33**	**y_4**		
187.14+2	y_3+2	**260.20**	**y_2**	333.71+2	b_6+2	508.31	a_6-NH_3		

Complete structural characterization and high identification coverage (81%) of the amino acid sequence of the α_1 subunit were obtained using nano-LC-FTMS mapping of peptide mixtures as a result of proteolytic degradation with trypsin (Table 4).

Table 4. Sequence coverage of the α_1 subunit of the $GABA_AR$ based on accurate masses and isotopic distribution.

Coverage based on accurate masses and isotopic distribution	Amount of identified amino acids	Total number of amino acids	Coverage, %
$[M+H]^{1+}$	214	455	47
$[M+2H]^{2+}$	47	455	10
$[M+3H]^{3+}$	40	455	9
$[M+4H]^{4+}$	64	455	14
$[M+5H]^{5+}$	6	455	1
Total coverage	371	455	81
Definitive tandem identification	214	455	47
Tandem consistent identification	117	455	26
Not yet analyzed	40	455	9

Most peptides have been identified as single charged peptides (47 %, 214 from 455 amino acids), some as doubly (10 %, 47 from 455 amino acids), about 9-14 % (40-64 from 455 amino acids) as triply and quadra charged peptides. Only 1 % (6 from 455 amino acids) of peptides existed in penta charged state. These data show that most peptides exist as singly and doubly charged peptides. Definitive tandem identification has been shown for 47 % of peptides, which means that about 80-90 % of the total set of **b-** and **y**–ions have been found. Tandem consistent identification has been found for 26 % (117 from 455 amino acids) of peptides, meaning that about 60 % of total **b-** and **y**-ions have been identified for each peptide's sequence. Based on MS/MS data, we calculated the sequence coverage of the different domains of α_1 subunit (Table 5).

Table 5. Identification of the sequence coverage of the α_1 subunit of the $GABA_AR$ extracellular and transmembrane domains based on results of nano-LC-FTMS analysis.

Sequence	Start-end	Total number of amino acids	Number of amino acids covered	Coverage, %
N-terminal	1-249	249	214	85
M1-domain	250-270	21	21	100, 00
M1-M2 Linker	271-276	6	6	100, 00
M2-domain	277-297	21	20	95
M3-M4 Linker	331-419	88	75	85
M3-domain	308-330	23	0	0, 00
M2-M3 Linker	298-307	10	0	0, 00
M4-domain	419-441	23	21	91
C-terminus	442-453	12	12	100, 00

The N-terminal and the C-terminus, which are extracellular domains, have been identified with extensive sequence coverage, 85 (214 from 249 amino acids) and 100 %, respectively. Other soluble domains, including the M1-M2 linker and M3-M4 linker, have also been determined with 100 and 85 % (75 from 88 amino acids), respectively. In contrast, the M2-M3 linker has not been identified because there are just two cleavage sites for trypsin at this peptide, at R (arginine, 299) and at K (lysine, 304). Therefore, trypsin degradation produces two peptides, one with very low molecular mass, $_{300}$NSLP$_{303}$. It is under the limit of nano-LC-FTMS detection. The second peptide is $_{305}$VAYATMDWFIAVCYAFVFSALIEFATVNYFT$_{335}$; its size is too big for nano-LC-FTMS detection. Soluble M3-M4 linker has been identified on 85 %, but it also contains the undetermined small peptide $_{389}$SATIEP$_{394}$. Transmembrane domains, including M1, M2, and M4, were determined almost completely, except for the M3 domain. M3 domain includes about 32 amino acids; its size and molecular mass are too big to be detected by MS/MS analysis. We design the map of the primary structure of the GABA$_A$R of the α_1 subunit (Figure 4 a and b).

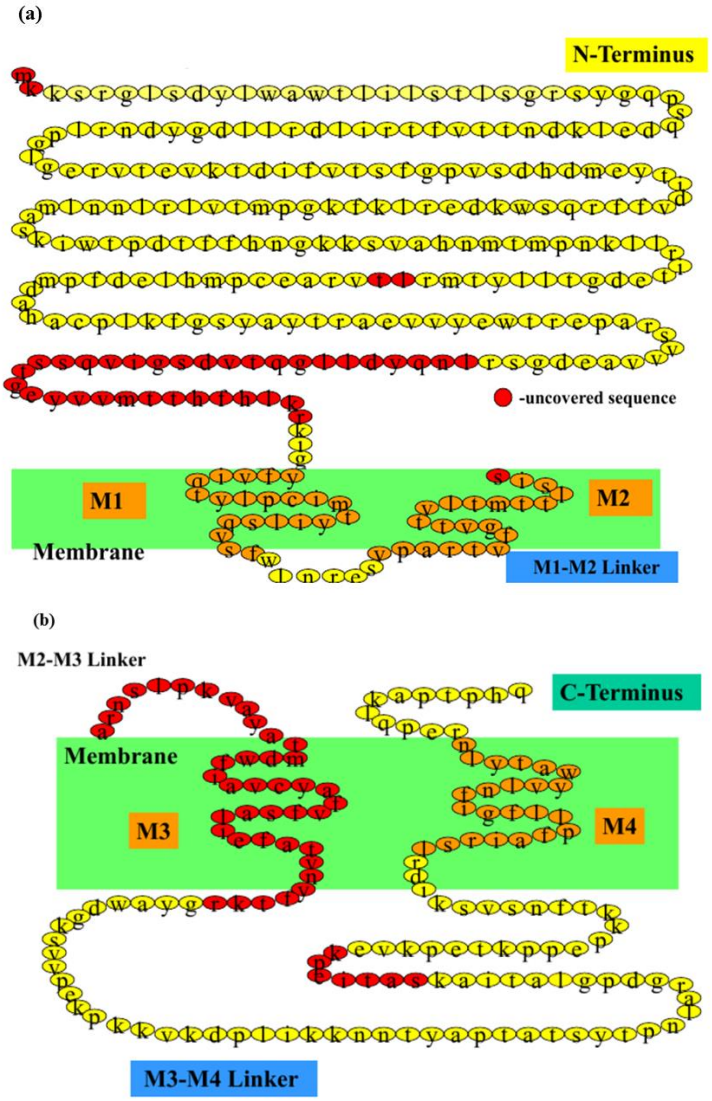

Figure 4. Coverage mapping of the α_1 subunit of the GABA$_A$R deduced from nano-LC-FTMS data: (**a**)-N-terminus, (**b**)-C-terminus. Identified amino acids (yellow and orange circles) and non-identified (red circles). The green color shows the hydrophobic part of the membrane.

Yellow and orange colored circles show a covered sequence of the α_1 subunit of the $GABA_AR$ from rat brain, but red colored circles show uncovered amino acid residues.

4. Conclusions

It has been established that γ-aminobutyric acid (GABA) is the main neurotransmitter in the central nervous system of mammals [40]. It is known that GABA plays a key role in the regulation of signaling to neurons in the brain, thereby affecting various physiological and psychological processes [41,42]. Changes in GABA levels have been shown to affect the development of various nervous and mental diseases [43-45]. It is known that GABA exerts its action through the ionotropic $GABA_A$ receptor [46-48]. This $GABA_A$ receptor is the target of many important drugs that affect GABAergic function and is widely used in the treatment of various neurological disorders such as anxiety, epilepsy, insomnia, spasms, aggressive behavior, stress, and other pathophysiological nervous and mental conditions and diseases [49-55]. Evidence from experimental and clinical studies indicates that $GABA_AR$ plays an important role in the mechanism and treatment of epilepsy [56]. This $GABA_AR$ is critical for brain development and function. Altered GABAergic transmission is thought to be associated with neurodevelopmental disorders. Subunit Shisa7 was recently identified as a $GABA_AR$ accessory subunit that modulated $GABA_AR$ transport and GABAergic transmission. It has been shown that a phosphorylation site critical for Shisa7-dependent $GABA_AR$ delivery contributes to behavioral endophenotypes seen in neurodevelopmental disorders. A phosphorylation site critical for Shisa7-dependent $GABA_AR$ delivery has been shown to influence behavioral endophenotypes in neurodevelopmental disorders.

Specifically, these mice exhibited hyperactivity, increased self-grooming, and impaired sleep homeostasis [57]. Earlier studies have shown that mutations in several $GABA_AR$ genes cause severe developmental disorders and the appearance of epileptic encephalopathies [58]. Analyzes of cell expression systems and mouse models show that all modifications in $GABA_AR$ genes cause loss of $GABA_AR$ function, which causes GABAergic disinhibition [59]. Recently, genetic studies have revealed the crucial role of the GABAergic system in the pathogenesis of various forms of epilepsy. The study of post-translational modifications of GABAergic receptor subunits provides an opportunity to develop precise therapeutic strategies that will be free from the burden of side effects observed with the use of GABAergic drugs. In our work, we identified post-translational modifications of the $GABA_AR$ of the α_1 subunit peptides from the rat brain, such as phosphorylation of serines, threonines, and tyrosines residues, oxidation of methionine and carbamidomethylation of cysteine. It should be emphasized that the determination of post-translational modifications is important for understanding the regulation of various $GABA_AR$ isoforms [60]. Currently available pharmacotherapeutic agents for the treatment of schizophrenia are not effective enough to restore the damaged cognitive functions observed in this disease. Thus, the search for more effective drugs continues. Allosteric modulation of the α_5 $GABA_AR$ subunit has been shown in animal models of schizophrenia, which is an effective tool for reversing the activity of the dopamine system [61]. Therefore, these α_5 $GABA_AR$ agonists are promising due to their potential to improve cognitive deficits in schizophrenia.

Of particular importance are drugs that affect and modulate the activity of the $GABA_AR$ complex, such as neuroactive steroids, benzodiazepines, barbiturates, various intravenous and inhalation anesthetics, and ethanol.

Molecular interactions and subsequent pharmacological effects caused by drugs acting on $GABA_AR$ are extremely complex due to the structural heterogeneity of the $GABA_AR$ and numerous allosterically binding sites of different ligands [62]. Currently, there is interest in the research and development of drugs that are selective with respect to the subunits of the $GABA_AR$, in particular, of the drugs that will be more effective and without side effects.
Regulation of $GABA_AR$ through post-translational modifications of receptor subunits may open up new prospects for developing specific drugs and developing new therapeutic approaches and methods for treating neurological diseases.
In turn, the study of post-translational modifications of the $GABA_AR$ subunits is necessary for understanding the regulation of receptor activity and its modulation by drugs necessary for brain functioning [63-68].

Thus, in this study, we isolated the $GABA_AR$ from small amounts of brain tissue, almost completely identified the primary structure of the α_1 subunit, and showed post-translational modifications of the peptides. It is possible that complete sequence coverage and detection of additional modification sites can be obtained using alternative proteolytic enzymes.

Taken together, our findings suggest that our comprehensive MS-based peptide mapping strategy is a sensitive and powerful method that will aid in the study of the structure of membrane proteins and receptors, as well as their post-translational modifications and ligand binding sites. A deep understanding of the structure and post-translational modifications of the $GABA_AR$ subunits will give a clear idea of the changes that can lead to CNS disorders. On this basis, these studies are vital for drug discovery and development in the future.

Funding

This research was funded by the Ministry of Science and Higher Education of the Russian Federation and performed under the state task, state registration #AAAA-A19-119071890015-6.

Acknowledgments

The authors are grateful to Bespalova O.O., an engineer at IPCP RAS (Chernogolovka, Moscow region, Russia), for technical assistance in preparing this publication.

Conflicts of Interest

The authors declare no conflict of interest. The funders had no role in the study's design, in the collection, analyses, or interpretation of data, in the writing of the manuscript, or in the decision to publish the results.

References

1. Maramai, S.; Benchekroun, M.; Ward, S.E.; Atack, J.R. Subtype Selective γ-Aminobutyric Acid Type A Receptor ($GABA_AR$) Modulators Acting at the Benzodiazepine Binding Site: An Update. *J Med Chem* **2020**, *63*, 3425-3446, https://doi.org/10.1021/acs.jmedchem.9b01312.
2. Field, M.; Dorovykh, V.; Thomas, P.; Smart, T.G. Physiological role for $GABA_A$ receptor desensitization in the induction of long-term potentiation at inhibitory synapses. *Nat Commun* **2021**, *12*, 2112, https://doi.org/10.1038/s41467-021-22420-9.
3. Kim, J.J.; Hibbs, R.E. Direct Structural Insights into $GABA_A$ Receptor Pharmacology. *Trends Biochem Sci* **2021**, *46*, 502-517, https://doi.org/10.1016/j.tibs.2021.01.011.

4. Sawyer, G.W.; Chiara, D.C.; Olsen, R.W.; Cohen, J.B. Identification of the bovine gamma-aminobutyric acid type A receptor alpha subunit residues photolabeled by the imidazobenzodiazepine [^{3}H] Ro15-4513. *J Biol Chem* **2002**, *277*, 50036-45, https://doi.org/10.1074/jbc.M209281200.
5. Sakai, S.; Tabuchi, K.; Murashita, H.; Hara, A. Activation of the GABA(A) receptor ameliorates the cochlear excitotoxicity caused by kainic acid in the guinea pig. *Tohoku J Exp Med* **2008**, *215*, 279-85, https://doi.org/10.1620/tjem.215.279.
6. Aller, M.I.; Paniagua, M.A.; Pollard, S.; Stephenson, F.A.; Fernandez-Lopez, A. The GABA(A) receptor complex in the chicken brain: immunocytochemical distribution of alpha 1- and gamma 2-subunits and autoradiographic distribution of BZ1 and BZ2 binding sites. *J ChemNeuroanat* **2003**, *25*, 1-18, https://doi.org/10.1016/s0891-0618(02)00071-6.
7. Mueller, P.J.; Fyk-Kolodziej, B.E.; Azar, T.A.; Llewellyn-Smith, I.J. Subregional differences in $GABA_A$ receptor subunit expression in the rostral ventrolateral medulla of sedentary versus physically active rats. *J Comp Neurol* **2020**, *528*, 1053-1075, https://doi.org/10.1002/cne.24798.
8. Olsen, R.W.; Bureau, M.H.; Endo, S.; Smith, G. The $GABA_A$ receptor family in the mammalian brain. *Neurochem. Res* **1991**, *16*, 317-325, https://doi.org/10.1007/BF00966095.
9. Chudomel, O.; Herman, H.; Nair, K.; Moshé, S.L.; Galanopoulou, A.S. Age- and gender-related differences in GABAA receptor-mediated postsynaptic currents in GABAergic neurons of the substantia nigra reticulata in the rat. *Neuroscience* **2009,** *163*,155-67. https://doi.org/10.1016/j.neuroscience.2009.06.025.
10. Kuhlemann, A.; Beliu, G.; Janzen, D.; Petrini, E.M.; Taban, D.; Helmerich, D.A.; Doose, S.; Bruno, M.; Barberis, A.; Villmann, C.; Sauer, M.; Werner, C. Genetic Code Expansion and Click-Chemistry Labeling to Visualize GABA-A Receptors by Super-Resolution Microscopy. *Front Synaptic Neurosci* **2021**, *13*, 727406, https://doi.org/10.3389/fnsyn.2021.727406.
11. Yang, W.; Drewe, J.A.; Lan, N.C. Cloning and characterization of the human $GABA_A$ receptor alpha 4 subunit: identification of a unique diazepam-insensitive binding site. *Eur.J. Pharmacol* **1995**, *291*, 319-325, https://doi.org/10.1016/0922-4106(95)90072-1.
12. Fan, P.C.; Lai, T.H.; Hor, C.C.; Lee, M.T.; Huang, P.; Sieghart, W.; Ernst, M.; Knutson, D.E.; Cook, J.; Chiou, L.C. The α6 subunit-containing GABAA receptor: A novel drug target for inhibition of trigeminal activation. *Neuropharmacology.* **2018**, *140*, 1-13, https://doi.org/10.1016/j.neuropharm.2018.07.017.
13. Sadamitsu, K.; Shigemitsu, L.; Suzuki, M.; Ito, D.; Kashima, M.; Hirata, H. Characterization of zebrafish GABAA receptor subunits. *Sci Rep* **2021**, *11*, 6242, https://doi.org/10.1038/s41598-021-84646-3.
14. Wingrove, P.; Hadingham, K.; Wafford, K.; Kemp, J.A.; Ragan, C.I.; Whiting, P. Cloning and expression of a cDNA encoding the human GABAA receptor alpha 5 subunit. *Biochem. Soc. Trans* **1992**, *20*, 18S, https://doi.org/10.1042/bst020018s.
15. Hipp, J.F.; Knoflach, F.; Comley, R.; Ballard, T.M.; Honer, M.; Trube, G.; Gasser, R.; Prinssen, E.; Wallace, T.L.; Rothfuss, A.; Knust, H.; Lennon-Chrimes, S.; Derks, M.; Bentley, D.; Squassante, L.; Nave, S.; Nöldeke, J.; Wandel, C.; Thomas, A.W.; Hernandez, M.C. Basmisanil, a highly selective GABAA-α5 negative allosteric modulator: preclinical pharmacology and demonstration of functional target engagement in man. *Sci Rep.* **2021**, *1*, 7700, https://doi.org/10.1038/s41598-021-87307-7.
16. Sears, S.M.; Hewett, S.J. Influence of glutamate and GABA transport on brain excitatory/inhibitory balance. *Exp Biol Med (Maywood).* **2021**, *246*, 1069-1083, https://doi.org/10.1177/1535370221989263.
17. Barker, J.S.; Hines, R.M. Regulation of GABAA Receptor Subunit Expression in Substance Use Disorders. *Int J Mol Sci.* **2020**, *21*, 4445, https://doi.org/10.3390/ijms21124445.
18. Walters, J.J.; Grayson, M.A.; Gross, M.L.; Hughes, M.; Shearer, G.; Kohel, D.H.; Baskin, J. Ion-exchange chromatography followed by ESI-MS for quantitative analysis of sugar monophosphates from glucose catabolism. *J Am Soc Mass Spectrom* **2006**, *17*, 104-107, https://doi.org/10.1016/j.jasms.2005.10.004.
19. Chalmers, M.J.; Hakansson, K.; Johnson, R.; Smith, R.; Shen, J.; Emmett, M.R.; Marshall, A.G. Protein kinase A phosphorylation characterized by tandem Fourier transform ion cyclotron resonance mass spectrometry. *Proteomics* **2004**, *4*, 970-981, https://doi.org/10.1002/pmic.200300650.
20. Pritchett, D.B.; Sontheimer, H.; Shivers, B.D.; Ymer, S.; Kettenmann, H.; Schofield, P.R.; Seeburg, P.H. Importance of a novel GABAA receptor subunit for benzodiazepine pharmacology. *Nature(Lond.)* **1989**, *338*, 582-585, https://doi.org/10.1038/338582a0.
21. Sakimoto, Y.; Oo, P.M.; Goshima, M.; Kanehisa, I.; Tsukada, Y.; Mitsushima, D. Significance of GABAA Receptor for Cognitive Function and Hippocampal Pathology. *Int J Mol Sci* **2021,** *22*, 12456, https://doi.org/10.3390/ijms222212456.

22. Belelli, D.; Hales, T.G.; Lambert, J.J.; Luscher, B.; Olsen, R.; Peters, J.A.; Rudolph, U.; Sieghart, W. GABAA receptors in GtoPdb v.2021.3. *IUPHAR BPS Guide Pharm CITE.* **2021**, *3*, https://doi.org/10.2218/gtopdb/F72/2021.3.
23. Ghit, A.; Assal, D.; Al-Shami, A.S.; Hussein, D.E.E. GABAA receptors: structure, function, pharmacology, and related disorders. *J Genet EngBiotechnol* **2021**, *19*, 123, https://doi.org/10.1186/s43141-021-00224-0.
24. Petroff, O.A. GABA and glutamate in the human brain. *Neuroscientist* **2002**, *8*, 562-573, https://doi.org/10.1177/1073858402238515.
25. Pierce, S.R.; Germann, A.L.; Akk, G. Activation of the α1β2γ2L GABAA Receptor by Physiological Agonists. *Biomolecules* **2021**, *11*, 1864, 1-6, https://doi.org/10.3390/biom11121864.
26. Olsen, R.W. GABAA receptor: Positive and negative allosteric modulators. *Neuropharmacology* **2018**, *136*, 10-22, https://doi.org/10.1016/j.neuropharm.2018.01.036.
27. Yang, J.Q.; Yang, C.H.; Yin, B.Q. Combined the GABA-A and GABA-B receptor agonists attenuates autistic behaviors in a prenatal valproic acid-induced mouse model of autism. *Behav Brain Res* **2021**, *403*, 113094, https://doi.org/10.1016/j.bbr.2020.113094.
28. Paine, T.A.; Chang, S.; Poyle, R. Contribution of GABAA receptor subunits to attention and social behavior. *Behav Brain Res* **2020**, *378*, 112261, https://doi.org/10.1016/j.bbr.2019.112261.
29. Hosie, A.M.; Wilkins, M.E.; da Silva, H.M.; Smart, T.G. Endogenous neurosteroids regulate GABAA receptors through two discrete transmembrane sites. *Nature* **2006**, *444*, 486-489, https://doi.org/10.1038/nature05324.
30. Sapp, D.W.; Witte, U.; Turner, D.M.; Longoni, B.; Kokka, N.; Olsen, R.W. Regional variation in steroid anesthetic modulation of [35S]TBPS binding to gamma-aminobutyric acid A receptors in rat brain. *J.Pharmacol.Exp.Ther* **1992**, *262*, 801-808, PMID: 1323664.
31. Poltl, A.; Hauer, B.; Fuchs, K.; Tretter, V.; Sieghart, W. Subunit composition and quantitative importance of GABA (A) receptor subtypes in the cerebellum of mouse and rat. *J. Neurochem* **2003**, *87*, 1444-1455, https://doi.org/10.1046/j.1471-4159.2003.02135.x.
32. Thompson, C.L.; Tehrani, M.H.; Barnes, E.M. Ir.; Stephenson, F.A. Decreased expression of GABAA receptor alpha6 and beta3 subunits in stargazer mutant mice: a possible role for brain-derived neurotrophic factor in the regulation of cerebellar GABAA receptor expression? *Mol. Brain Res* **1998**, *60*, 582-290, https://doi.org/10.1016/s0169-328x(98)00205-8.
33. Laemmli, U.K. Cleavage of structural proteins during the assembly of the head of bacteriophage T4. *Nature* **1970**, *227*, 680-685, https://doi.org/10.1038/227680a0.
34. Shevchenko, A.; Jensen, O.N.; Podtelejnikov, A.V.; Neubauer, G.; Shevchenko, A.; Mortensen, P.; Mann, M. A strategy for identifying gel-separated proteins in sequence databases by MS alone. *Proc. Natl.Acad.Sci* **1996**, *93*, 14440-14445, https://doi.org/10.1042/bst0240893.
35. Cordido, A.; Vizoso-Gonzalez, M.; Nuñez-Gonzalez, L.; Molares-Vila, A.; Chantada-Vazquez, M.D.P.; Bravo, S.B.; Garcia-Gonzalez, M.A. Quantitative Proteomic Study Unmasks Fibrinogen Pathway in Polycystic Liver Disease. *Biomedicines*, **2022**, *10*, 290. https://doi.org/10.3390/biomedicines10020290.
36. Clauser, K.R.; Baker, P.; Burlingame, A.L. Role of accurate mass measurement (+/- 10 ppm) in protein identification strategies employing MS or MS/MS and database searching. *Anal.Chem* **1999**, *71*, 2871-2882, https://doi.org/10.1021/ac9810516.
37. Stancliffe, E.; Schwaiger-Haber, M.; Sindelar, M.; Patti, GJ. DecoID improves identification rates in metabolomics through database-assisted MS/MS deconvolution. *Nat Methods* **2021**, *18*, 779-787, https://doi.org/10.1038/s41592-021-01195-3.
38. Feng, S.; Sterzenbach, R.; Guo X. Deep learning for peptide identification from metaproteomics datasets. *J Proteomics* **2021**, *247*, 104316, https://doi.org/10.1016/j.jprot.2021.104316.
39. Yang, Y.; Horvatovich, P.; Qiao, L. Fragment Mass Spectrum Prediction Facilitates Site Localization of Phosphorylation. *J Proteome Res* **2021**, 20, 634-644, https://doi.org/10.1021/acs.jproteome.0c00580.
40. Li, H.; Heise, K.F.; Chalavi, S.; Puts, N.A.J.; Edden, R.A.E.; Swinnen, S.P. The role of MRS-assessed GABA in human behavioral performance. *ProgNeurobiol* **2022**, *212*, 102247, https://doi.org/10.1016/j.pneurobio.2022.102247.
41. Salihu, S.; MeorAzlan, N.F.; Josiah, S.S.; Wu, Z.; Wang, Y.; Zhang, J. Role of the cation-chloride-cotransporters in the circadian system. *Asian J Pharm Sci* **2021**, *16*, 589-59, https://doi.org/10.1016/j.ajps.2020.10.003.

42. Shao, F.B.; Fang, J.F.; Wang, S.S.; Qiu, M.T.; Xi, D.N.; Jin, X.M.; Liu, J.G.; Shao, X.M.; Shen, Z.; Liang, Y.; Fang, J.Q.; Du, J.Y. Anxiolytic effect of GABAergic neurons in the anterior cingulate cortex in a rat model of chronic inflammatory pain. *Mol Brain* **2021**, *14*, 139, https://doi.org/10.1186/s13041-021-00849-9.
43. Zuo, W.; Zhao, J.; Zhang, J.; Fang, Z.; Deng, J.; Fan, Z.; Guo, Y.; Han, J.; Hou, W.; Dong, H.; Xu, F.; Xiong, L. MD2 contributes to the pathogenesis of perioperative neurocognitive disorder via the regulation of α5GABAA receptors in aged mice. *J Neuroinflammation* **2021**, *18*, 204, https://doi.org/10.1186/s12974-021-02246-4.
44. Gammon, D.; Cheng, C.; Volkovinskaia, A.; Baker, G.B.; Dursun, S.M. Clozapine: Why Is It So Uniquely Effective in the Treatment of a Range of Neuropsychiatric Disorders? *Biomolecules* **2021**, *11*, 1030, https://doi.org/10.3390/biom11071030.
45. Rafiee, F.; RezvaniHabibabadi, R.; Motaghi, M.; Yousem, D.M.; Yousem, I.J. Brain MRI in Autism Spectrum Disorder: Narrative Review and Recent Advances. *J MagnReson Imaging* **2022**, *55*, 1613-1624, https://doi.org/10.1002/jmri.27949.
46. Antoni, F.A. The Case for Clinical Trials with Novel GABAergic Drugs in Diabetes Mellitus and Obesity. *Life (Basel)* **2022**, *12*, 322, https://doi.org/10.3390/life12020322.
47. Dannenhoffer, C.A.; Spear, L.P. Excitatory/inhibitory balance across ontogeny contributes to age-specific behavioral outcomes of ethanol-like challenge in conditioned taste aversion. *Dev Psychobiol* **2019**, *61*, 1157-1167, https://doi.org/10.1002/dev.21864.
48. Sallard, E.; Letourneur, D.; Legendre, P. Electrophysiology of ionotropic GABA receptors. *Cell Mol Life Sci* **2021**, *78*, 5341-5370, https://doi.org/10.1007/s00018-021-03846-2.
49. Rao, R.; Shah, S.; Bhattacharya, D.; Toukam, D.K.; Cáceres, R.; PomeranzKrummel, D.A.; Sengupta, S. Ligand-Gated Ion Channels as Targets for Treatment and Management of Cancers. *Front Physiol* **2022**, *13*, 839437, https://doi.org/10.3389/fphys.2022.839437.
50. Xia, G.; Han, Y.; Meng, F.; He, Y.; Srisai, D.; Farias, M.; Dang, M.; Palmiter, R.D.; Xu, Y.; Wu, Q. Reciprocal control of obesity and anxiety-depressive disorder via a GABA and serotonin neural circuit. *Mol Psychiatry* **2021**, *26*, 2837-2853, https://doi.org/10.1038/s41380-021-01053-w.
51. Jafarian, M.; Modarres Mousavi, S.M.; Rahimi, S.; GhaderiPakdel, F.; Lotfinia, A.A.; Lotfinia, M.; Gorji, A. The effect of GABAergic neurotransmission on the seizure-related activity of the laterodorsal thalamic nuclei and the somatosensory cortex in a genetic model of absence epilepsy. *Brain Res* **2021**, *1757*, 147304, https://doi.org/10.1016/j.brainres.2021.147304.
52. El-Mallakh, R.S.; Ali,Z. Extra-synaptic modulation of GABAA and efficacy in bipolar disorder. *Med Hypotheses* **2021**, *147*, 110501, https://doi.org/10.1016/j.mehy.2021.110501.
53. Sun, T.Y.; Ma, L.X.; Mu, J.D.; Zhang, Z.; Yu, W.Y.; Qian, X.; Tian, Y.; Zhang, Y.D.; Wang, J.X. Acupuncture improves the structure of spastic muscle and decreases spasticity by enhancing GABA, KCC2, and $GABA_A\gamma 2$ in the brainstem in rats after ischemic stroke. *Neuroreport* **2022**, *33*, 399-407, https://doi.org/10.1097/WNR.0000000000001798.
54. Jager, A.; Amiri, H.; Bielczyk, N.; van Heukelum, S.; Heerschap, A.; Aschrafi, A.; Poelmans, G.; Buitelaar, J.K.; Kozicz, T.; Glennon, J.C. Cortical control of aggression: GABA signalling in the anterior cingulate cortex. *Eur Neuropsychopharmacol* **2020,** *30*, 5-16, doi: 10.1016/j.euroneuro.2017.12.007
55. Crombie, G.K.; Palliser, H.K.; Shaw, J.C.; Hodgson, D.M.; Walker, D.W.; Hirst, J.J. Effects of prenatal stress on behavioural and neurodevelopmental outcomes are altered by maternal separation in the neonatal period. *Psychoneuroendocrinology* **2021**, *124*, 105060, https://doi.org/10.1016/j.psyneuen.2020.105060.
56. Maljevic S, Møller RS, Reid CA, Pérez-Palma E, Lal D, May P, Lerche H. Spectrum of $GABA_A$ receptor variants in epilepsy. *Curr Opin Neurol.* **2019**, *32*, 183-190. https://doi.org/10.1097/WCO.0000000000000657.
57. Wu, K.; Han, W.; Tan,Q.;Li,Y.;Lu,W. Activity- and sleep-dependent regulation of tonic inhibition by Shisa7. *Cell Rep* **2021,** *34*, 108899. doi: 10.1016/j.celrep.2021.108899.
58. Gunn, B.G.; Cunningham, L.; Mitchell, S.G.; Swinny, J.D.; Lambert, J.J.; Belelli, D. $GABA_A$ receptor-acting neurosteroids: a role in the development and regulation of the stress response. *Front Neuroendocrinol* **2015**, *36*, 28-48, https://doi.org/10.1016/j.yfrne.2014.06.001.
59. Janzen, D.; Slavik, B.; Zehe, M.; Sotriffer, C.; Loos, H.M.; Buettner, A.; Villmann, C. Sesquiterpenes and sesquiterpenoids harbor modulatory allosteric potential and affect inhibitory $GABA_A$ receptor function *in vitro*. *J Neurochem* **2021**, *159*, 101-115, https://doi.org/10.1111/jnc.15469.

60. Soghomonian, J.J.; Gonzales, C.; Chesselet, M.F. Messenger RNAs encoding glutamate-decarboxylases are differentially affected by nigrostriatal lesions in subpopulations of striatal neurons. *Brain Res* **1992**, *576*, 68-79, https://doi.org/10.1016/0006-8993(92)90610-l.
61. Gill KM, Grace AA. The role of α5 $GABA_A$ receptor agonists in the treatment of cognitive deficits in schizophrenia. *Curr Pharm Des.* **2014**, *20*, 5069-76. https://doi.org/10.2174/1381612819666131216114612
62. Jembrek MJ, Vlainic J. GABA Receptors: Pharmacological Potential and Pitfalls. *Curr Pharm Des.* **2015**, *21*, 4943-59, https://doi.org/10.2174/1381612821666150914121624.
63. Chaibi, I.; Bennis, M.; Ba-M'Hamed, S. GABA-A receptor signaling in the anterior cingulate cortex modulates aggression and anxiety-related behaviors in socially isolated mice. *Brain Res* **2021**, *1762*, 147440, https://doi.org/10.1016/j.brainres.2021.147440.
64. Nagy, J.; Ebbinghaus, B.; Hoon, M.; Sinha, R. $GABA_A$ presynaptic inhibition regulates the gain and kinetics of retinal output neurons. *Elife.* **2021**, *10*, e60994. https://doi.org/10.7554/eLife.60994.
65. Joshi, S.; Kapur, J. Neurosteroid regulation of $GABA_A$ receptors: A role in catamenial epilepsy. *Brain Res* **2019**, *1703*, 31-40, https://doi.org/10.1016/j.brainres.2018.02.031.
66. Baldassarro, V.A.; Sanna, M.; Bighinati, A.; Sannia, M.; Gusciglio, M.; Giardino, L.; Lorenzini, L.; Calzà, L. A Time-Course Study of the Expression Level of Synaptic Plasticity-Associated Genes in Un-Lesioned Spinal Cord and Brain Areas in a Rat Model of Spinal Cord Injury: A Bioinformatic Approach. *Int J Mol Sci* **2021**, *22*, 8606, https://doi.org/10.3390/ijms22168606.
67. Mehta, A.; Shirai, Y.; Kouyama-Suzuki, E.; Zhou, M.; Yoshizawa, T.; Yanagawa, T.; Mori, T.; Tabuchi,K. IQSEC2 Deficiency Results in Abnormal Social Behaviors Relevant to Autism by Affecting Functions of Neural Circuits in the Medial Prefrontal Cortex. *Cells* **2021**, *10*, 2724, https://doi.org/10.3390/cells10102724.
68. Kiemes, A.; Gomes, F.V.; Cash, D.; Uliana, D.L.; Simmons, C.; Singh, N.; Vernon, A.C.; Turkheimer, F.; Davies, C.; Stone, J.M.; Grace, A.A.; Modinos, G. $GABA_A$ and NMDA receptor density alterations and their behavioral correlates in the gestational methylazoxymethanol acetate model for schizophrenia. *Neuropsychopharmacology* **2022**, *47*, 687-695, https://doi.org/10.1038/s41386-021-01213-0.